AN EXTREMELY LOW ESR AND ESL ANNULAR FILM CAPACITOR

By:

T. A. Hosking
M. A. Brubaker
SBE, Inc.

Abstract

Across the industry, the traditional approach to input circuit design of Large Switching Power Systems is the use of bulk storage Aluminum Electrolytic Capacitors in parallel with banks of High Frequency Bypass Film Capacitors. SBE Inc. has developed an innovative new approach to address problems typically associated with this method. SBE has designed a single annular form factor dry film capacitor, which simultaneously addresses the bulk storage and ripple current requirement. This novel solution allows for a low profile bus structure and inherently results in extremely low ESR and ESL. A design is presented along with data on the Ripple Current Capability, ESR and ESL as well as other system level thermal management simplification possibilities.

Introduction

An annular form factor dry film capacitor has been developed to simultaneously address energy storage and ripple current requirements for large switching power systems. Traditionally, energy storage for such systems has been provided by aluminum electrolytic capacitors with parallel high frequency bypass film capacitors to handle the ripple current. While the idea of using film capacitors to replace electrolytic devices is not new, the annular capacitor is unique in that a single part replaces a parallel bank of standard form factor capacitors. The annular capacitor can sustain higher operating voltages than comparable electrolytic components with significantly lower losses. Furthermore, the annular form factor is optimal for dissipation of internal heating and the temperature rise will be relatively small even for ripple currents exceeding 500 A at frequencies on the order of 100 kHz. With the heating contribution of the capacitor significantly reduced, the designer is left to focus upon heat removal from semiconductors, inductors and current carrying structures. The user must recognize that external heating due to losses in the bus structure may ultimately determine the capacitor hot spot temperature.

This paper presents an 1800 μF annular dry film capacitor design with discussion of the associated thermal modeling. Details of a resonant ripple current test stand are provided along with preliminary temperature profile data for capacitors with asymmetrical and symmetrical contact arrangements. The two-dimensional finite element results are compared with the experimental data for the latter case. External heating from the bus structure is demonstrated to dominate the capacitor temperature profile relative to internal losses for currents up to 150 A at 100 kHz.

Annular Capacitor Design

The 1800 μF annular capacitor utilizes 6-micron polypropylene film metallized with a zinc alloy to obtain a worst-case sheet resistance of 6 Ω/square. The 62.5 mm wide film is wound on a polystyrene hollow core having a respective inner and outer diameter of 75 mm and 85 mm. A polyester tape wrap is applied after winding and the nominal outer diameter of the capacitor is 304.8 mm (12 inches). End connections are made by end spray with an initial layer of zinc followed by an additional layer of tin/zinc alloy. Various contact arrangements are connected to the end spray using a suitable silver epoxy. A typical capacitor mounted in the ripple current test fixture is shown in Figure 1.

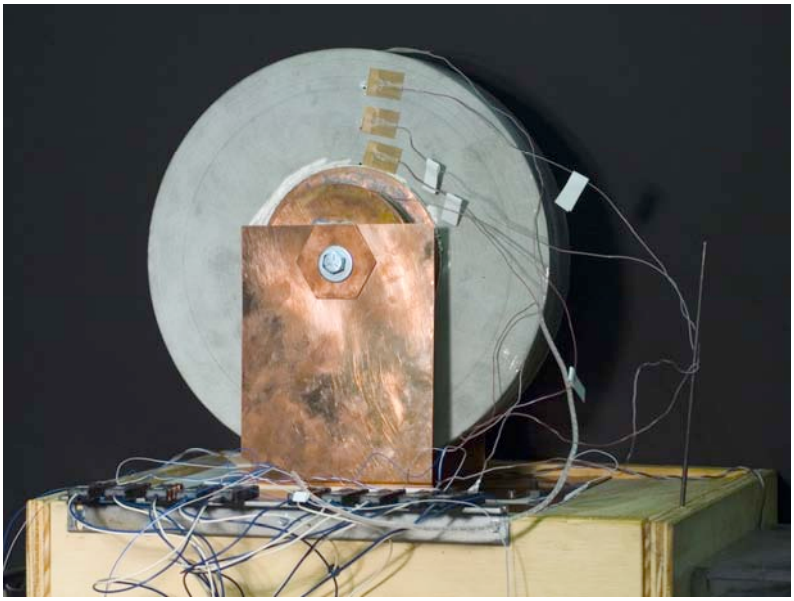

Figure 1. A typical 1800 μF annular capacitor mounted in ripple current test fixture.

An optimistic equivalent series inductance (ESL) for the capacitor can be estimated assuming a round conductor on the capacitor axis connecting the electrodes to form a discharge path. For a 1" diameter conductor, the ESL will be approximately 26.5 nH. While this number is valid for the capacitor, the total ESL in a practical circuit will ultimately be defined by the connection geometry, which cannot be specified by the capacitor vendor. The equivalent series resistance (ESR) can be readily estimated assuming that losses in the metallized electrodes will dominate over dissipation in the dielectric. For this case, the capacitor internal ESR will be less than 50 μΩ, but the resistance of the end spray may be significant depending upon the contact arrangement at the system level.

Thermal Modeling

Traditional thermal design formulas for film capacitors are semi-empirical relationships that in many cases were developed before cost effective computer simulations became available. The use of finite element analysis for modeling of capacitors can provide a significant step forward in understanding and optimizing thermal designs. The Flux2D^{TM} [1] software package was obtained to support steady-state, two-dimensional thermal simulation with the ability to incorporate anisotropic materials, temperature dependent thermal properties, and boundary conditions for convection and radiation.

Finite element modeling of the capacitor winding is rather difficult due to the difference in length scale between the film (microns), metallization (nanometers) and winding (mm). Two approaches have been developed, namely a lumped region model and an anisotropic bulk material model. In the first case, layers of film and foil are lumped together such that the total volume of each is preserved. Even with this approach, additional scaling based on a constant conductivity-thickness product is required to achieve workable dimensions. In contrast, the anisotropic method creates a new material based on the series and parallel combination of the film and metallization thermal resistances. While both methods have been demonstrated to be valid using a computationally intensive base case, the anisotropic approach is much easier to implement and has been independently demonstrated by other investigators [2].

In the radial direction, the total thermal resistance through a layer of metallized film will be the series combination of the thermal resistance for each material given as:

$$R_T = \frac{L}{kA}$$

where L is the length in the direction of heat transfer, A is the cross sectional area and k is the thermal conductivity. Recognizing that k is three orders of magnitude larger and L is three orders of magnitude lower for the metallization with the same area for both materials, the film will dominate in the radial direction such that $k_r = k_{PP}$. Looking in the axial direction, the thermal resistances will combine in parallel and the effective thermal conductivity will be:

$$k_z = k_{PP} + \frac{t}{d} k_{metallize}$$

where t and d are the respective metallization and film thickness. For the film used on the prototype annular capacitor, the axial thermal conductivity will be about two times the radial value, which has a significant effect upon the heat transfer.

All of the materials used in the capacitor have thermal conductivities that vary to some degree with temperature. For the end spray, the published properties of tin and zinc are combined to approximate the "as sprayed" material, recognizing that the oxide layers between metal droplets may have an effect. There is very little published data regarding the thermal conductivity of polypropylene film over temperature. However, recent work by NIST suggests that the thermal conductivity will increase substantially for temperatures approaching 100^{o}C [3]. A linear fit to the NIST data was used for the polypropylene and combined with typical data for the metallization bulk materials to estimate $k_z(T)$.

The thermal behavior of a film capacitor is quite complex with spatially distributed heating contributions from resistive losses in the electrodes, dissipation in the dielectric, resistive losses in the end spray and resistive losses in the leads. Models for each of these mechanisms can be readily developed and superimposed in the finite element domain in the form of power densities. For the ripple current application, the applied RMS voltage is small, and dielectric loss can be neglected. Losses at the contact points between the end spray and film metallization are acknowledged, but cannot readily be quantified [4].

The metallized electrode losses vary along the axial length of the capacitor in a parabolic fashion with the maximum occurring at the margin and the minimum at the center. This can be readily understood by considering the capacitive current distribution for one electrode. At the edge facing the other electrode across the margin, there will be no current flow. Moving axially away from this edge; the current increases linearly with capacitance. The maximum current is realized at the opposite margin, and remains constant moving out to the end spray. The power density will thus be quadratic over the active width in the form:

$$P/V = \frac{4\mathring{a}^2 z^2}{d^2 t}\left(\frac{I_o}{C_o}\right)^2 R_s$$

where ε is the permittivity, z is the axial distance from the edge with zero current, d is the film thickness, t is the metallization thickness, R_s is the sheet resistance and I_o is the total current flowing through the total capacitance C_o. In order to account for air between layers and other practical winding effects, the permittivity must be scaled by a "K" factor that typically ranges from 0.85-0.95. For a given layer, the two electrodes have the same distribution starting at opposite ends, and the superposition weighting each contribution by _ gives a parabola with the minimum at the axial center point as described above. This result is consistent with other derivations [4], but is often ignored when calculating temperature rise based on total losses. For the anisotropic winding model described above, the power density must be referred to the film thickness and the t variable in the previous equation is replaced with the film thickness d. In the margins, the effective width of the film (EWF) is substituted for z. Note that there is no variation in the radial direction for the electrode loss.

For the annular form factor design, the end spray losses will become significant due to the large end face area. The losses will be highly dependent upon the nature of the lead configuration used to connect the capacitor the external circuit. An annular contact arrangement is clearly better with the radius optimized such that the currents in the end spray on the inside and outside are equal. To better understand this situation, consider first the limiting cases where the contact is at the inner or outer radius of the winding. In the former case, the power density will be:

$$P/V = \frac{1}{4\partial^2 r^2 a}\left[\frac{r_2^{\,2} - r^2}{r_2^{\,2} - r_1^{\,2}}\right]^2 I_o^{\,2} R_s$$

where a is the end spray thickness, r_1 is the inner radius of the capacitor winding, r_2 is the outer radius of the capacitor winding and r is the radius. From the form of this equation, it is clear that the power density increases very quickly as r approaches r_1. At this point, the end spray is carrying all of the current through an annular resistance that increases logarithmically as r decreases. A similar result can be obtained for the contact at r_2 with the numerator of the

bracketed term modified to be r^2-r_1^2. With the contact located at $r_1 < r_c < r_2$, the limiting case results can be utilized for the inner and outer annular sections with r_c replacing r_1 or r_2 in the numerator of the bracketed term. The lowest losses will be realized for the case where r_c is such that the capacitances on both sides of the contact are balanced.

The axisymmetric finite element domain used for initial analysis of the ring capacitor is presented in Figure 2.

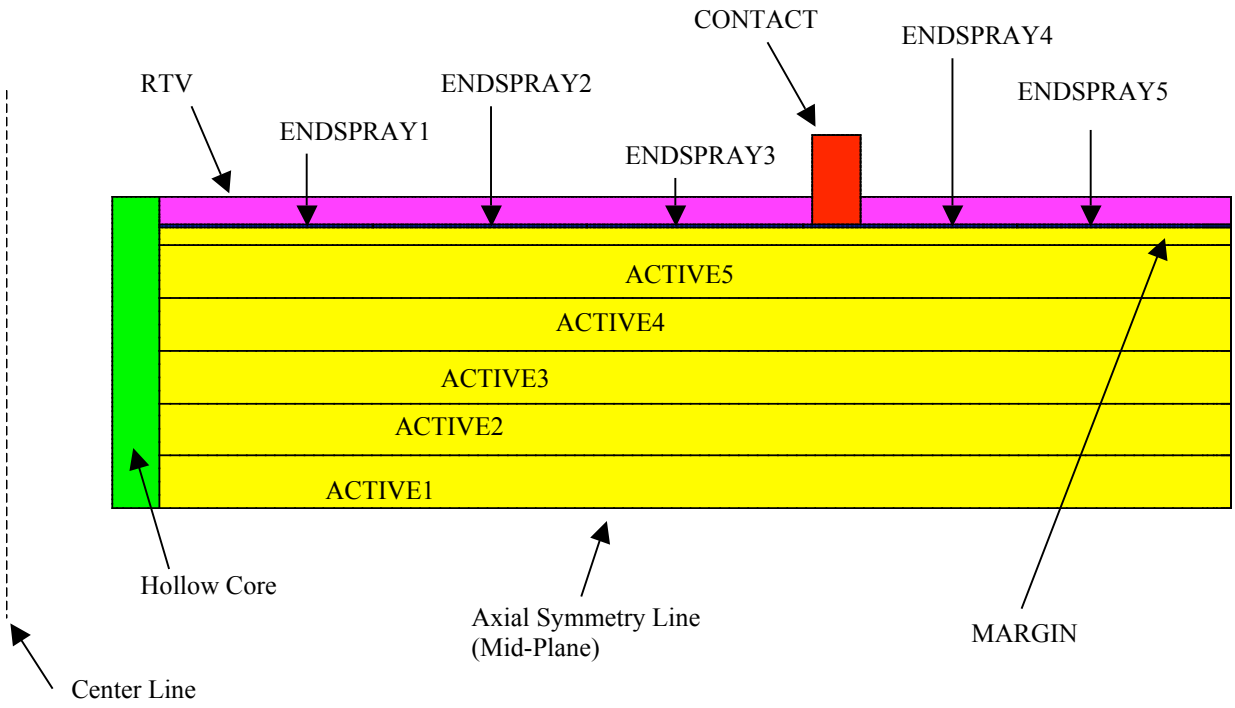

Figure 2. Illustration of finite element domain for thermal analysis

Half symmetry is assumed about the z-axis and the mid-plane of the capacitor. In order to account for spatially distributed losses, the end spray and active volume are segmented into sections that can be assigned individual power densities. The end spray region is composed of five sections of equal annular thickness that have different volumes. The half of the active volume in the domain is divided into five sections of equal volume. The source region power densities for the active volume and end spray regions are presented respectively for a 500 A current at 100 kHz in Figure 3 and Figure 4. Note that the dielectric dissipation is negligible since a very low voltage is applied to drive the current at this frequency. The importance of contact radius is illustrated through the comparison of various cases for the end spray power density.

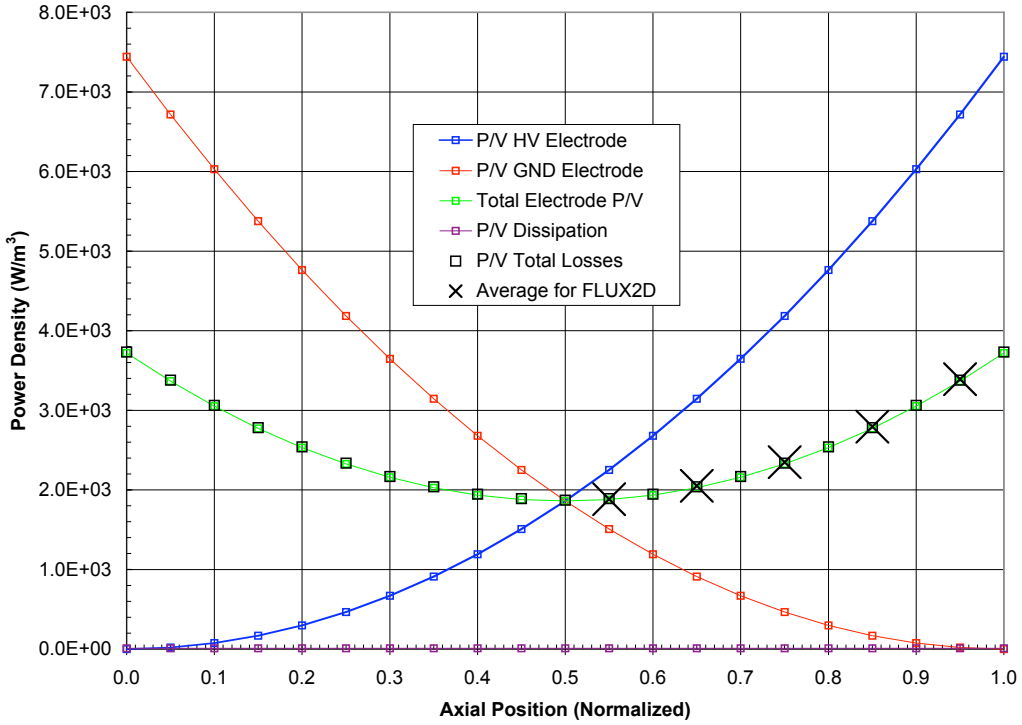

Figure 3. Axial distribution of power density due to losses in the capacitor winding

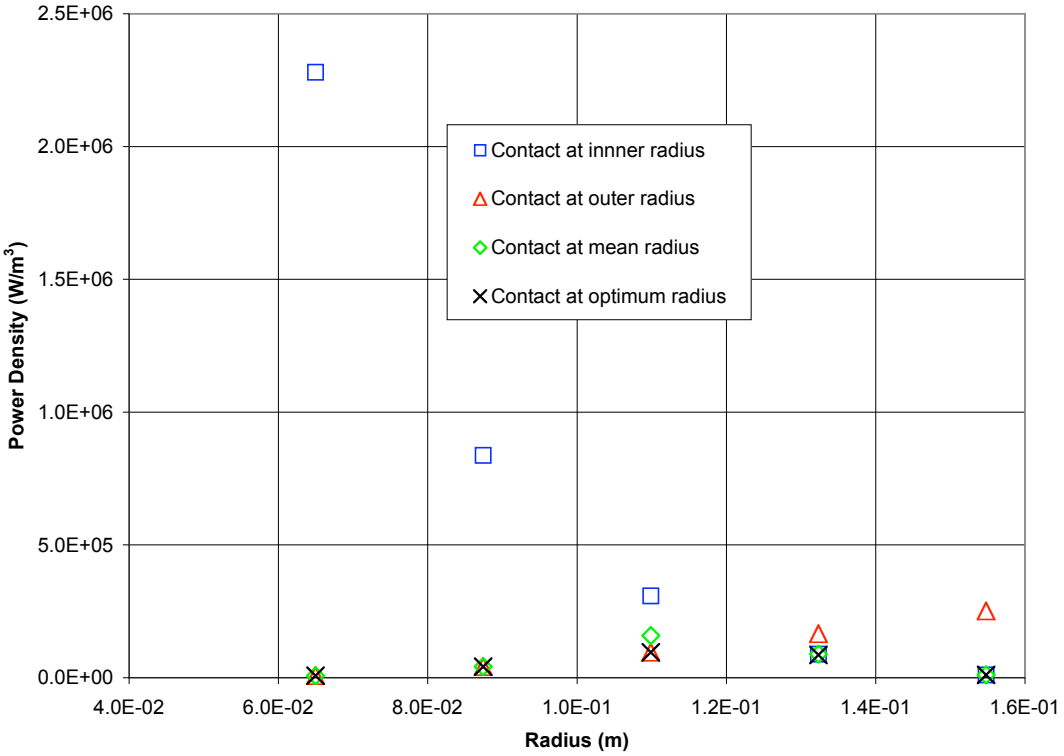

Figure 4. Power density distribution across the end spray due to resistive losses

The end face and outer surface of the capacitor were treated as exchange boundaries having an emissivity of 0.5 and a convection heat transfer coefficient of 5, which is reasonable for free (natural) convection [5]. A Dirichlet boundary was applied across the end face of the contact and all other domain boundaries were set to a Neumann condition such that isotherms must be normal to the surface. With the contact and ambient temperature for the exchange boundary set to 25°C, the temperature profile for the 500 A case at 100 kHz is presented in Figure 5 with the contact at the optimal location. The total losses are on the order 7 W, but the capacitor aspect ratio allows excellent heat transfer such that the total rise at the hot spot is only 5.5 degrees.

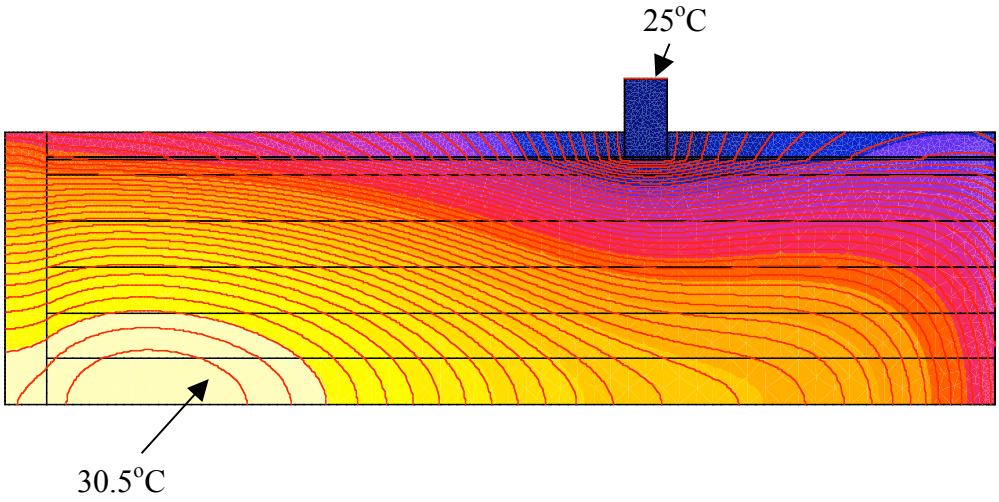

Figure 5. Thermal profile for 500 A case at 100 kHz with optimal contact position.

Test Arrangement

A resonant test setup was assembled to support ripple current testing of large value annular capacitors at 100 kHz as illustrated in Figure 6.

Figure 6. Photograph of the ripple current test stand

The sinusoidal waveform was provided by a function generator driving the input of an ENI 1500W RF power amplifier. The amplifier output was connected across a coil that was inductively coupled through free space to a 0.9 μH inductor. A capacitor bank of 2.8 μF in series with the 1800 μF test capacitor was connected across the inductor terminals. The small capacitance dominates the resonance such that the frequency was 100 kHz. The turns ratio and coupling coefficient were adjusted to match the amplifier output impedance of 50 Ω. The capacitor was mounted vertically above the inductor box and exposed only to free convection combined with air currents due to ventilation in the building. Temperature measurements were obtained using J-type thermocouples selected with a rotary switch for readout on an Omega 199 controller. Surface measurements were made along the end face in the radial direction with adhesive probes. Measurements at the mid-plane were obtained by inserting probes into small holes drilled from the end face and distributed in the radial direction. Note that the capacitors were electrically cleared via applied voltage after drilling the holes.

Comparison of Theoretical and Experimental Results

Initial testing was conducted using a prototype ring capacitor that was already available with contacts located on only one location on the outside of the ring. While clearly not an optimal configuration, this sample was useful to take some initial data and verify the test stand design. Significant heating was observed in the end spray due to the asymmetrical current flow through the long path to the bus as expected. Additional prototypes were fabricated with a symmetric contact arrangement as shown in Figure 1 and Figure 6. An illustration comparing the symmetric and asymmetric current distributions for the different contact cases is provided in Figure 7.

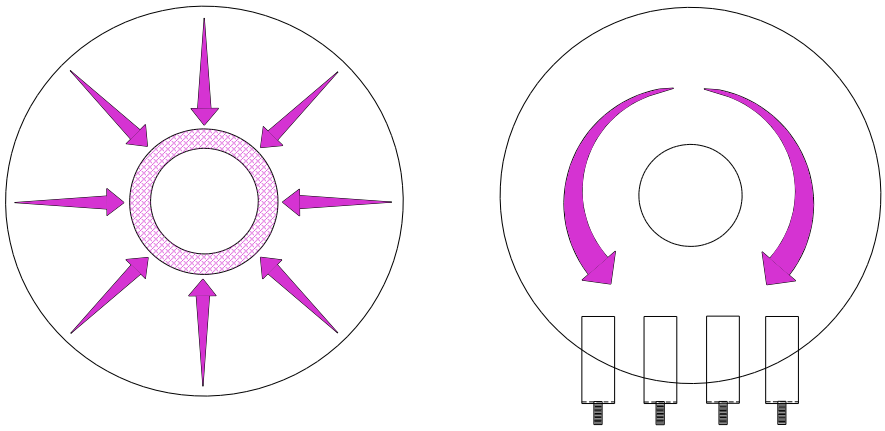

Figure 7. Illustration of end spray current distribution for symmetric and asymmetric contact schemes

The symmetric contact was comprised of a copper ring soldered to a standard 4” pipe and then bonded to the capacitor end face with silver epoxy. The contact radius for this case is not optimal, but was viewed as useful to obtain preliminary data for a symmetrical geometry to compare with the finite element results. The pipe section was one inch long and terminated with a flat copper plate soldered to the end and bolted to a section of copper flashing running vertically from the bus. An identical arrangement was used on both sides of the capacitor.

With the symmetrical arrangement, bus heating was found to dominate the thermal profile with the contact radius being smaller than the optimal case. The measured and calculated steady state temperature profiles on the capacitor mid-plane and end face are compared in Figure 8 for currents of 100 A and 150 A at 100 kHz. The measured surface temperature half way along the axis of the pipe contact was used to provide a reference temperature for the finite element model. In order to improve the fit, the heat transfer coefficient for the convection boundary conditions was reduced from 5 to 2, which is still reasonable for free convection. A first order calculation based on the Grashov number for a vertical flat plate of length scale comparable to the capacitor predicts a heat transfer coefficient in the range of 1.7 to 2.2 based on accepted empirical data [5]. Neglecting internal heating in the capacitor simulation changes the temperature profile by less than one degree. Thus, it is clear that the capacitor is simply acting to cool the bus structure and is not the limiting factor for determining how much ripple current can be sustained in the test setup.

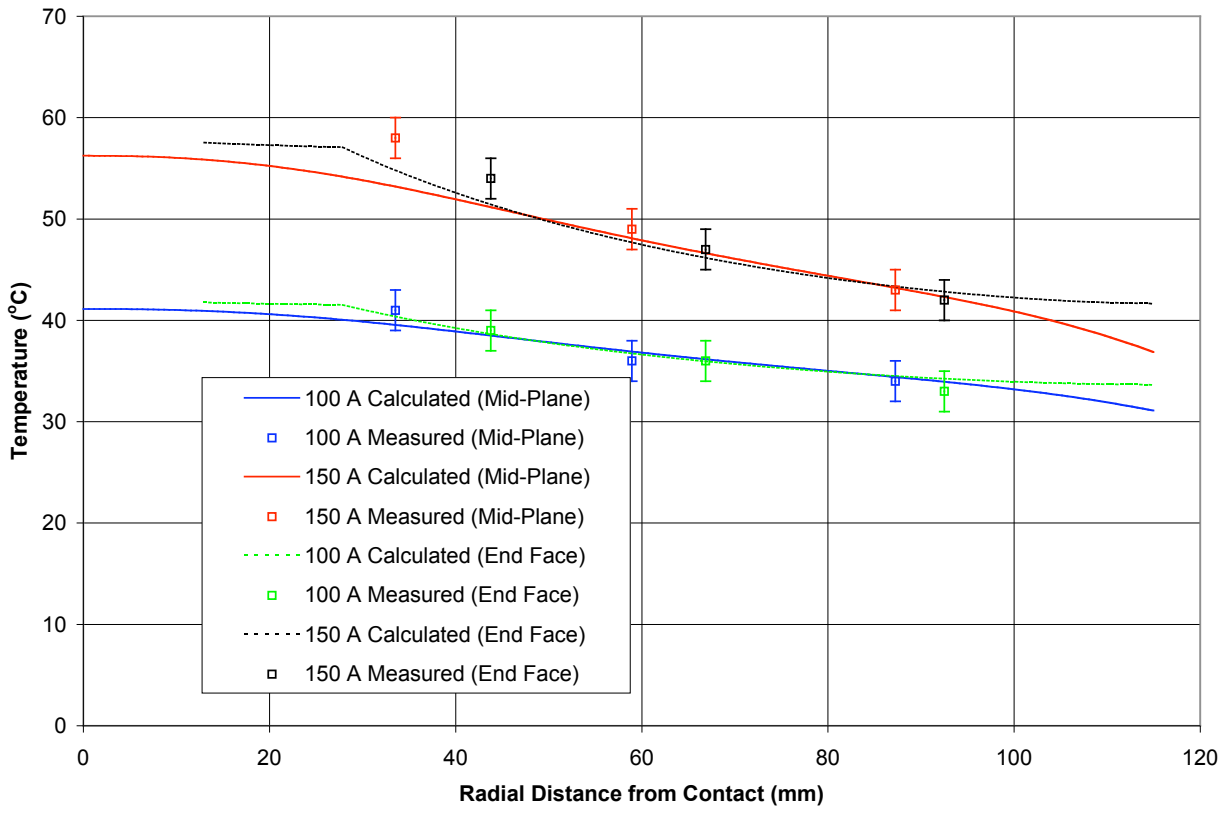

Figure 8. Comparison of calculated and measured temperature profiles for 100 kHz ripple current with an 1800 μF capacitor having a symmetrical contact

Conclusions

The annular form factor dry film capacitor offers an excellent solution for switching power supplies with energy storage and high frequency bypass functionality combined into a single package. Experimental results indicate that bus heating dominates the capacitor hot spot temperature for currents up to 150 A at 100 kHz. Excellent correlation between the experimental and theoretical results has been demonstrated and the finite element model suggests that currents exceeding 500 A can be readily handled with proper thermal design of the bus structure.

The symmetrical contact scheme presented here was selected specifically for the purpose of comparing the model and experimental data and is not intended to represent an optimal configuration for a real application. Having established a solid correlation, various terminal options can now be evaluated to take advantage of the extremely low ESR for the annular capacitor. The end user must recognize that the capacitor thermal performance may ultimately be limited by the contact configuration and bus structure rather than internal losses. Future work will address measurement and modeling for currents exceeding 300 A with consideration of current rating as a function of the number and location of terminals subject to mechanical restrictions in practical systems.

References

[1] Flux2D™ distributed by Magsoft Corporation, 20 Prospect Street, Ballston Spa, New York 12020.

[2] M. H. El-Husseini et al, "Thermal Simulation for Geometric Optimization of Metallized Polypropylene Film Capacitors", IEEE Trans. Industry Applications, Vol. 38, No. 3, May/June 2002, pp 713-718.

[3] T. Kashiwagi et al, "Thermal and Flammability Properties of Polypropylene/Carbon Nanotube Nanocomposites", Polymer 45 (2004) 4227-4239, Elsevier.

[4] S. Boggs et al, "Analysis of the Effects of End Connection Quality on the Dielectric Loss of Metallized Film Capacitors", IEEE Trans. Dielectrics and Electrical Insulation, Vol. 11, No. 6, December 2004, pp 990-994.

[5] F. P Incropera and D. DeWitt, Introduction to Heat Transfer 2nd Edition, Wiley, 1990.

NOTES

Who we are:

For over 45 years world-class quality film capacitors have been designed and manufactured at our facility in Barre, Vermont. The ubiquitous Orange Drop® has been the cornerstone of technology for SBE, having served the electronics industry since 1959. Formerly a Sprague Electric company, SBE has built on that rich history with a renewed focus on providing application specific capacitor solutions.

Technology and Innovation:

SBE has developed innovative and unique technologies to address demanding requirements in the fields of pulse power, high voltage and high power density. Several patents have already been filed in these areas to support the growing challenges that designers of power electronics face today. SBE has worked with companies such as TASER™, DRS Optronics, Northrop Grumman and Los Alamos to provide technology solutions where conventional products fail.

The Power Ring™:

SBE's technology roadmap continually pushes us to think "outside the box". As part of our E^2P^2 – Extreme Energy/Pulse Power™ technology division, we have launched the distinctive Power Ring™ dry film capacitor series that is specifically tailored to each application. No longer are system designers forced to work around fixed dimensions. The Power Ring now offers the designer flexibility like never before.

Experience and Teamwork:

The SBE team is focused on building on the critical success factors that keep us competitive today. Proactive desire to cross-train, weekly production "point team" meetings that track all aspects of WIP, entire plant floor accountability for on-time delivery, set-up reduction programs to reduce leadtimes, and the sharing of productivity metrics and how they affect cost. This culture, combined with our desire to lead with technology, provides the core make-up of SBE.

SBE, Inc. • 131 South Main Street
Barre, Vermont 05641-4854 USA
Tel: 802-476-4146
Fax: 802-476-4149
Web: www.SBElectronics.com
E-mail: Info@SBElectronics.com